



This is a repository copy of *The development of a new artificial model of a finger for assessing transmitted vibrations.*

White Rose Research Online URL for this paper:
<http://eprints.whiterose.ac.uk/124768/>

Version: Accepted Version

Article:

Almagirby, A., Rongong, J.A. orcid.org/0000-0002-6252-6230 and Carré, M.J. (2018) The development of a new artificial model of a finger for assessing transmitted vibrations. *Journal of the Mechanical Behavior of Biomedical Materials*, 78. pp. 20-27. ISSN 1751-6161

<https://doi.org/10.1016/j.jmbbm.2017.11.005>

Article available under the terms of the CC-BY-NC-ND licence
(<https://creativecommons.org/licenses/by-nc-nd/4.0/>).

Reuse

This article is distributed under the terms of the Creative Commons Attribution-NonCommercial-NoDerivs (CC BY-NC-ND) licence. This licence only allows you to download this work and share it with others as long as you credit the authors, but you can't change the article in any way or use it commercially. More information and the full terms of the licence here: <https://creativecommons.org/licenses/>

Takedown

If you consider content in White Rose Research Online to be in breach of UK law, please notify us by emailing eprints@whiterose.ac.uk including the URL of the record and the reason for the withdrawal request.



eprints@whiterose.ac.uk
<https://eprints.whiterose.ac.uk/>

The development of a new artificial model of a finger for assessing transmitted vibrations

*Almaky Almagirby, Jem A. Rongong and Matt J. Carré

Department of Mechanical Engineering, The University of Sheffield, Sheffield UK

Abstract

Prolonged exposure of the hand to tool-induced vibrations is associated with the occurrence of conditions such as vibration white finger. This study involves the development of a new artificial model that approximates both loading and vibration behaviour of the human finger. The layered system uses polypropylene “bones”, encased in a cylinder of low modulus, room-temperature curing silicone gel (to replicate subcutaneous tissues), with an outer layer of latex (to replicate the dermis and epidermis). A protocol for manufacture was developed and dynamic mechanical analysis was carried out on a range of gels in order to choose a range close to the mechanical properties of the human finger. The load-deflection behaviour under quasi-static loading was obtained using an indenter. The indentation measurements were then compared with a set of validation data obtained from human participant testing under the same conditions. A 2-D FE model of the finger was also used to assess vibration responses using existing parameters for a human finger and those obtained from the tested materials. Vibration analysis was conducted under swept sinusoidal excitations ranging from 10-400 Hz whilst the FE finger model was pressed 6 mm toward the handle. Results were found to compare well. This synthetic test-bed and protocol can now be used in future experiments for assessing finger-transmitted vibrations. For instance, it can aid in assessing anti-vibration glove materials without the need for human subjects and provide consistent control of test parameters such as grip force.

Keywords: Vibration white finger; Dynamic mechanical analysis; Finger mechanical properties; Artificial finger, Finite element modelling; Finger-transmitted vibration

1. Introduction

The prolonged usage of vibrating hand-held tools, in an operator's daily work routine is associated with the development of hand-arm vibration syndrome (HAVS). Vibration-induced finger damage and disorders are recognised as a major aspect of HAVS (Griffin, 1990), and the fingers are important substructures within the hand-arm system. The evaluation of anti-vibration (AV) gloves should be partly based on the amount of vibration reduction on the fingers (Paddan et al., 2001). However, mainly due to technical challenges, the measurement of the vibration transmissibility of the AV gloves at the fingers has been very limited (Griffin et al., 1982; Paddan et al., 2001). Possibly for similar reasons, the AV glove evaluation standard uses the vibration transmissibility of the glove on the palm of the hand and in the forearm direction (ISO 10819, 1996; 2013) but not on the fingers. This standard does not directly attempt to resolve the challenge of vibration attenuation at the fingers. However, the original version included criteria which required that any AV glove had to be a full-finger glove with similar materials and thickness at both the palm as well as the fingers (ISO 10819, 1996). Subsequently, the required thickness of the glove material at the fingers has been relaxed from 100% to greater than or equal to 55% of the thickness of the palm in the revised version of the glove standard (ISO 10819, 2013).

The measurement of the vibration transmissibility of gloves can be affected by many factors, such as: variability between and within subjects (Hewitt 1998; Paddan et al., 2001), controlling feed and grip forces, test rig behaviour, and temperature. One previous study has investigated the effects of several variables on measuring vibration transmissibility of gloves; it has found that misalignment of the palm-adaptor can reduce the measured transmissibility by approximately 20%. Other variables include inter-subject variability ($\pm 10\%$), temperature variation ($\pm 4\%$) and controlling feed forces ($\pm 4\%$) (Hewitt 1998).

Measurements of glove transmissibility at the fingers are limited and require more research (Paddan et al., 2001). One of the existing methods uses a finger-adaptor (similar to the standard palm-adaptor) method to measure the glove transmissibility at the fingers. Unfortunately, the effectiveness of transmissibility measured using this method can be overestimated for assessing gloves due to a number of factors including: the difficulty of using the adaptor inside the glove; and the effective mass of each finger being small compared to that of the palm. Also, the geometry and the mass of the finger is relatively small when compared to the probable geometry and mass of the finger-adaptor. The effectiveness with which gloves reduce the vibration transmission at the finger would be better if the transmissibility was measured reliably (Welcome et al., 2014). Further, the vibration transmissibility measured at the finger can vary depending on the location of the measurement on each of the fingers (Welcome et al., 2011). It is therefore difficult to use the finger-adaptor method to evaluate the transmissibility distribution reliably. Additionally, the glove transmissibility at the fingers can be indirectly estimated by measuring vibrations for gloved and un-gloved fingers (Cheng et al., 1999; Paddan et al., 2001). A modelling study indicated that using a relative method is acceptable for estimating the transmissibility at the finger-glove interface (Dong et al., 2009). However, using the finger-adaptor method may change the geometry of the finger which may

affect the dynamic properties of the finger and produce unreliability in measurement (Concettoni et al., 2009).

Several recent studies have used a 3-D laser vibrometer for measuring the transmissibility at the back of the fingers, and using such a technique reduced the unreliability associated with the use of the finger adaptor method (Welcome et al., 2011; Dong, 2013; Welcome et al., 2014; Welcome et al., 2015). However, no in-vivo experimental method has been established that directly measures the vibration responses inside the soft tissues of the hand-arm system (ISO 5349-1, 2001; Wu et al., 2010); their evaluation remains dependent on modelling, and the accuracy of the models is based on how accurate the data is which is used. Finite element modelling (FE) is considered to be the best method for providing detailed biodynamic responses inside the soft tissues of the entire system, and several studies have investigated the FE model that replicates the biodynamic responses of the human finger to vibration (Wu et al., 2007; Wu et al., 2008; Wu et al., 2010; Wu et al., 2015).

The mechanical properties of human skin differ and can be influenced by a number of factors including hydration, age and anatomical structure (Derler et al., 2007; Shao et al., 2009). This variability creates a complication when attempting to obtain consistent and reliable results from individuals. To achieve a reliable measurement which produces the mechanical behaviour of human skin, such as the friction and stiffness properties of human skin, synthetic models of a fingertip have been created for experimental use (Derler et al., 2007; Shao et al., 2009), but none of these studies have included vibration transmission.

Several materials have been investigated for replicating human skin and soft tissue structures at the fingertip. In a previous study a synthetic model was created using polyvinylsiloxane (Ramkumar et al., 2003a; b). Another study has used various silicone and polyurethane materials as mechanical friction equivalents to the skin, and a polyurethane-coated polyamide fleece with a surface structure was found which is like that of skin and demonstrated the best friction correspondence to human skin in dry conditions (Derler et al., 2007). A recent study has used 101RF silicone rubber (cured hardness: 30 Shore A) to replicate the mechanical properties of the anatomical construction of the real fingertip. The results show that a synthetic fingertip that utilised only pure silicone showed a difference in friction behaviour when compared to the real fingertip. However, the soft multi-layer synthesis fingertip was found to be closer to the real one (Shao et al., 2009).

This present study was designed to develop and test a new physical model for assessing finger-transmitted vibration that can replicate the mechanical and vibration behaviour of the real human finger at room temperature.

2. Materials

2.1 Materials analysis

Two types of material were selected for analysis. Room-temperature curing silicone gel based on polyorganosiloxanes (Magic Power Gel, from Raytech, see Table 1 for details) was used to replicate subcutaneous tissues while latex (Liquid Latex Rubber, from Polycraft) was used to replicate the outer

layer skin (the dermis and epidermis). Two cylindrical specimens of silicone gel were prepared with two different mixing ratios by volume. One cuboid specimen of latex was cut from a cured sheet. A summary of the properties of the specimens is provided in Table 2

Table 1: The properties of Power Magic Gel

Components	Colour	Approx. working time	Cross linking time
Part A	transparent	7-10 minutes	10-15 minutes
Part B	blue		

Table 2: Properties and dimensions of the specimens used in the study

Material	No. of specimens	Mixing ratio	Dimensions (mm)
Silicone gel	2	1:1 and 1:2	H = 35.5, \varnothing = 20
Latex	1	-	H = 29.3, L = 20, W = 1.6

Dynamic Mechanical Analysis (DMA) was conducted to study the mechanical properties (Young's modulus and loss factor) of the selected material specimens and to investigate their sensitivity to temperature and amplitude changes. This information was used to determine the optimum mixing ratio of the silicone gel parts (base and catalyst) to provide a similar stiffness to that of the real human tissues.

DMA was performed using a Metravib Viscoanalyser, as shown in Figure 1 (a). The installation of each specimen varied, depending on the design of the specimen. Each of the silicone gel specimens (1:1 and 1:2) was inserted between compression plates that were located in an analyser chamber as shown in Figure 1 (b), whilst for the latex sheet specimen two clamps were used instead (see Figure 1 (c)). Specimens were subjected to sinusoidal loading and the resulting force and displacement traces used to find the Young's modulus and loss factor.

Each specimen was subjected to a strain sweep test at room temperature followed by a temperature sweep test. For the strain sweep test, each specimen was tested under different dynamic strain amplitudes at room temperature, whilst the temperature test was conducted under a fixed dynamic strain amplitude over a range of temperatures. The temperature of the specimen was measured using a thermocouple located inside the chamber. First, the chamber temperature was cooled down using liquid nitrogen until the target temperature was obtained, and then the specimen was subjected to sinusoidal loading with a selected dynamic strain. A frequency of 10 Hz was selected for all the tests and the specimens. The selection of the frequency was dependent on the calibration of the machine that showed the best dynamic response at 10 Hz and specimen size. The testing parameters are shown in Table 3.

Table 3: Parameters used for testing the specimens of materials

Test type	Strain sweep		Temperature sweep	
	Room temp., °C	Strain range	Temp. range, °C	Dynamic strain
Silicone gel	23.3	0.0001-0.01	0-40	0.003
Latex sheet	25.4	0.0001-0.01	5-40	0.002

In order to check the consistency of the silicone gel (Power Magic Gel) over time, the specimen of mix ratio 1:2 was retested under the same condition after 30 days. The 1:1 specimen was damaged during removal from DMA machine and this was not suitable for re-testing.

2.2 Geometry and parameters of an artificial finger (AF)

The anatomy and mechanical properties of the human index finger were considered in order to develop a physical model of the finger. The structure of the human finger is shown in Figure 4. The Young's modulus of tissues in the human finger was previously defined: for a bone ($E = 1.5 \times 10^9$ Pa), subcutaneous tissues ($E = 3.4 \times 10^4$ Pa) and skin, including (epidermis and dermis) ($E = 1.36 \times 10^5$ Pa) (Wagner et al., 2008). In the present study a polypropylene rod (nylon), 8 mm in diameter, provided by Plastic Direct Ltd, UK, was used to make artificial phalanx bones that had a Young's modulus similar to that of human phalanx bones (1.5×10^9 Pa).

2.3 Development and manufacture of an artificial finger (AF)

Silicone gel with a mixing ratio of 1:1.013 was used to replicate the subcutaneous tissues at room temperature. This mixing ratio was found using linear interpolation between the two values obtained from DMA of the two silicone specimens (1:1 and 1:2) at a room temperature of 23.3 °C. This predicted a Young's modulus of 3.4×10^4 Pa, matching the value used by Wagner et al., 2008.

First, three polypropylene phalanx bones were prepared with three different lengths to replicate the length of the distal, middle and proximal phalanges (15.82, 22.38 and 39.78 mm) (Alexander et al., 2010). These bones each had a 1.5 diameter hole along its axis, which made it possible to join them using nylon line (250 lb fishing line, 1.5 mm in diameter, from Blog Action Outdoor Ltd). Once positioned with the correct spacing between them that allowed bending but ensured the exact length of all three phalanges together, the bones were bonded to the line using cyanoacrylate adhesive (Krazy glue). The joined phalanx bones were then installed inside a metal mould (with inner diameter of 20 mm) prepared for this study. The metal mould had aluminium end-plates with 1.5 mm holes through which the nylon line joining the bones was anchored. The holes were offset 4 mm from the centre of the cavity to match the geometry of human finger (see Figure 2b).

The silicone components (at a ratio of 1:1.013) were mixed for about 1 minute. The resulting mixture was degassed within a degassing chamber until it was clear and transparent (bubble-free), and then poured into the mould and cured for 10 minutes. After that, the model was safely removed from the mould.

In order to study the effect of the thickness of the skin layer on both the static and dynamic behaviour of the finger model, five artificial models of the finger (AF) were produced: four of them used the same protocol utilised earlier while one used a 1:2 mixing ratio of silicone components for comparison.

Each of the five artificial models was then painted using liquid latex to replicate the outer layer of the human skin. Because the latex had a Young's modulus that was higher (1.8 MPa) than that of human skin (0.136 MPa), the thickness of the outer layer was varied between the five models. It was found that it was a challenge to obtain an accurate and homogeneous thickness of the outer layer. Therefore, the outer skin

layer of the models was imaged using Optical Coherence Tomography system (OCT), from VivoSight, which is usually used for skin research. The images were analysed using a Matlab algorithm (Matlab version R2015a) based on an analysis of the light reflectivity/backscatter profiles (A-scans) to obtain an accurate measurement of the thickness of the outer layer (Maiti et al., 2016). The characteristics of the artificial models used, are shown in Table 4.

Table 4: Characteristics of the five physical models of finger

Artificial Finger	Silicone gel	Latex skin thickness		Total mass	Length	Outer radius	Volume
	Mixing ratio	Mean, mm	SD, mm	grams	mm	mm	mm ³
AF1	1:1.013	1.202	0.055	40.9	102.4	11.2	40353
AF2	1:1.013	1.195	0.051	40.3	102.4	11.2	40297
AF3	1:1.013	0.616	0.040	36.2	101.2	10.6	35820
AF4	1:1.013	1.285	0.056	39.9	102.6	11.3	41019
AF5	1:2	0.299	0.024	35.6	100.6	10.3	33503

3. Method

3.1 Indentation measurements

Seventeen human participants, males aged 21 to 61 were used for the testing, and their characteristics are listed in Table 5. The experimental design was reviewed and approved by the Research Ethics Committee of the Faculty of Engineering at the University of Sheffield.

Table 5: Characteristics of the human participants

Variable	Mean	SD	Min.	Max.
Age (years)	40.47	14.01	21	61
Height (m)	1.77	0.07	1.63	1.95
Weight (kg)	76.09	9.85	60	91
Wrist circumference (mm)	175.88	9.92	163	196
Palm circumference (mm)	212.82	11.70	194	248
Hand size (BS EN 420:2003)	8.41	0.62	8	10
Length of finger (mm)	99.47	3.18	93	105
Indicative volume of finger (mm ³)	27257	4246	22812	35971

The length of the index finger was measured using a ruler with a length of 15 cm, as the distance from the fingertip to the metacarpophalangeal joint of the index finger. The indicative volume of the index finger (IV_{IF}) was found by assessing an average of the diameters of distal and proximal segments (IF_D). The volume was calculated using the following equation:

$$IV_{IF} = \frac{\pi L_{IF} IF_D^2}{4} \quad \text{Equation 3.1}$$

In order to study the load-deflection behaviour of the right index finger, a Mecmesin MDD test stand with a digital force gauge (see Figure 3a) was modified to be used horizontally, as shown as in Figure 3b. A

support base was attached to the main test stand. A cylindrical indenter made from polypropylene, 12.25 mm in diameter and 30 mm in length was attached to the digital force gauge (500 N limit). A displacement transducer (spring return linear sensor, 9615, BEI Sensors) was also included in the rig. This allowed force and displacement measurements to be recorded continuously using Lab View software version 2014, and via an NI USB-6002 DAQ card.

Each participant was subjected to a quasi-static loading at the proximal segment of the right index finger as shown as in Figure 5, b. In order to replicate posture when gripping, the proximal segment was measured with a bent finger. To ensure that all participants maintained the same posture, an aluminium finger supporter was made and attached to the test system (as shown in Figure 5, b). To remove any friction between the indenter and the skin that might affect the load-deflection behaviour of the finger, a water-based lubricant (Boots Lubricating Jelly) was applied to the indenter before each individual test began. Participants were instructed to remain in a relaxed posture during testing but it is possible that different participants with different strength capabilities, may have reacted differently during testing. Future studies will consider this aspect in the testing procedure.

The load-deflection behaviour of each of the five finger models was carried out using the same test rig and protocol that was used for human measurements. However, for the artificial models, the test rig was set up vertically instead, Figure 5 a.

3.2 Vibration analysis

3.2.1 Two-Dimensional Finite Element model (2D-FE) of proximal index finger:

The finger segment was considered to be composed of layers representing the skin (including epidermis and dermis), subcutaneous tissue and bone, as shown in Figure 4. The cross-sections of both the finger itself and the bone were considered circular, with external diameters of 20 and 8 mm respectively, while their centroids were offset by 4.27 mm, based on anthropometric measurement, X-ray and RM imaging (Eliot, 1991; Alexander et al., 2010; Dewangan et al., 2010; Wang et al., 2012). This offset resulted in the subcutaneous tissue having an asymmetric thickness around the bone. The skin however, was considered to have a constant thickness of 0.8 mm (Wu et al., 2006b; Dong et al., 2008). In this study, the finger was pressed against a rigid surface and the response to sinusoidal excitation over a range of frequencies obtained at the accelerometer location (the outer top point of the skin layer). The rigid surface was assumed to be aluminium and the contact between it and the skin layer was considered frictionless. As motion across the diameter of the finger was of primary interest, the model consisted of a 2D slice of the finger. Quadratic plane-strain elements (element type: CPE8R) were utilised in the mesh and analysis was conducted using the commercial software Abaqus (version 6.13).

Material properties used in the model are based on previous studies (Wu et al., 2006a; Wu et al., 2006b;

Dong et al., 2008; Wang et al., 2011; Wang et al., 2012) as summarised in Table 6. Both the bone and the aluminium surface were assumed to display isotropic, elastic behaviour. The soft tissues were considered to have linear hyperelastic and linear viscoelastic behaviour. The linear hyperelastic material is a type of constitutive model for elastic material for which the stress and strain relationship derives from a strain energy potential function (Neo-Hooke) whilst the linear viscoelastic material is that for which there is a linear relationship between stress and strain at any given time.

Table 6: Material properties used in modelling

Material	Density	Long term Young's modulus	Poisson's ratio	Structural damping
	kg/m ³	Pa		
Aluminium	2700	70×10 ⁹	0.33	0.0
Bone	1800	1.5×10 ⁹	0.33	0.0
Skin	1000	1.0×10 ⁵	0.48	0.6
Subcutaneous tissue	1000	3.4×10 ⁴	0.48	0.6

For the soft tissues, the hyperelastic (NeoHooke potential) and viscoelastic (Prony series)(Zheng et al., 1996) material parameters are shown in Tables 7 and 8 (Wu et al., 2006b) and were based on data obtained from published experimental work by fitting constitutive models to stress/strain and stress relaxation curves (Zheng et al., 1996; Pan et al., 1998).

Table 7: Hyperelastic and viscoelastic parameters for the skin

i	C_{10i} (MPa) ⁻¹	D_{1i} (MPa) ⁻¹	g_i	τ_i (s)
1	0.01689	2.4	0.0864	0.2136
2	0.0	0.0	0.2136	8.854

Table 8: Hyperelastic and viscoelastic parameters for the subcutaneous tissue

i	C_{10i} (MPa) ⁻¹	D_{1i} (MPa) ⁻¹	g_i	τ_i (s)
1	0.005743	7.059	0.2566	0.3834
2	0.0	0.0	0.2225	4.6731

The viscoelastic damping arising from these models is relatively low, with loss factors below 0.01 in the frequency range of interest, as they were originally developed for studying creep rather than vibration behaviour. To represent behaviour within the frequency range (10-400 Hz), structural damping was considered in this FE model for the skin and the subcutaneous tissue and ignored for bone and aluminium in this FE model (see Tables 7 and 8).

3.2.2 Simulation procedure:

In order to generate the frequency response of the finger pressed against a vibrating surface, the procedure was conducted in two steps. The first step involved a finite-strain, quasi-static analysis in which the nodes

at the centre of the bone were pressed by applying a concentrated force that allowed the nodes moving 6 mm towards the rigid surface. This was in order to obtain the static deformation behaviour of the finger model. In this static analysis, the geometry and material nonlinearities were considered, as the model consisted of three different layers. The second step was a steady-state, frequency domain analysis using infinitesimal strain assumptions starting from the state reached at the end of the first step. In this step, the rigid surface was assumed to oscillate over a frequency range from 10 to 400 Hz. The output from this step was the transmissibility at the location of the finger-mounted accelerometer (the outer top point of the skin layer) with reference to the handle. In the physical experiment, the mass of the accelerometer is 0.3 grams. In the 2D simulation where the cross-section depth used was 1 mm, the accelerometer mass therefore represented as a point mass of 0.06 grams that added to the outer top point of the skin layer.

4. Results

4.1 Results from DMA testing of materials

DMA result for the latex specimen are shown in Figure 5. The latex specimen showed Young's modulus values of around 1.8 MPa, typical of a rubbery polymer, which decreased somewhat with dynamic strains as well as with temperature. The loss factor was almost independent of dynamic strain and decreased slightly as the temperature increased.

The two silicone specimens showed insensitivity in both Young's modulus and loss factors to the dynamic strain levels and temperature changes, see Figure 6. The silicone specimen with 1:2 ratio (A:B) was about 5 times stiffer than the one with the 1:1 ratio.

The retest results of silicone specimen 1:2 did not show any significant change in the mechanical properties over an interval of 30 days, indicating the material is reasonable for medium-term lab use. The values of Young's modulus obtained from the silicone gel materials were found to be within the range of interest. In addition, any effects due to temperature changes within the range 0 to 40 °C are now known, which could have implications for conditions of testing and storage.

4.2 Stiffness measurements

The results obtained from indentation measurements from the finger model and the human index finger (proximal) were used to determine the stiffness at a given loading force by fitting a 4th order polynomial to the data and finding its derivative. The loading behaviour of the finger models and the human right index finger are shown in Figure 7.

The results showed that the artificial models appear to have similar loading behaviour to that in the human finger at low loading force ranging from 0-2 N, except AF5 which was developed with a different stiffness (5 times stiffer) for comparison. The AF3 model was found to be the closest to the human finger. It should be noted that the load-displacement behaviour for the finger models was found to vary among artificial fingers with similar stiffness of soft tissues, with the differences mostly depending on the skin thickness of the finger and the loading variance.

Table 9 shows the stiffness measured at loading forces of 5 and 10 N, for all five artificial fingers, as well as that obtained from human measurement. At the loading of 5 N, the stiffness was approximately two to three times lower in the artificial fingers than in that of the human proximal finger segment and about three to five times that of the human distal. The AF5 model was the stiffest due to the higher mixing ratio for the gel layer. The stiffness at the proximal was found to be doubled when the loading force of 10 N was applied. However, for the artificial models the stiffness increased by about double for all the fingers. This was mostly due to the geometry of the artificial finger layers which were designed as a uniform cylinder, which allowed an easier deflection than the human finger.

Table 9: Comparison of stiffness obtained from human testing and all five artificial models of finger

	Stiffness, N/mm					
	Human proximal	AF1	AF2	AF3	AF4	AF5
At 5 N	3.84±0.8	1.32	1.18	1.38	1.51	2.82
At 10 N	8.67±3.45	2.72	2.77	3.27	2.61	3.50

4.3 2D FE model validation of parameters from tested materials:

In this section, the FE model of the finger was used to validate the vibration behaviour of the artificial finger. The dynamic response was carried out for an FE model of the finger that used properties of the human finger (original FE model), followed by an FE model that used the properties of tested materials that were used to develop the artificial finger (latex and silicone gel). Both models were pressed from the bone towards the rigid surface by 6 mm in order to simulate the effect of the maximum gripping on finger-transmitted vibration. The transmissibility measurement showed that both FE models were found to have similar behaviour at frequencies up to 120 Hz. The FE model that simulated human data was found to resonate at a slightly lower frequency to the FE model that used the tested materials (190 and 198 Hz respectively). This is possibly due to Young's modulus of the skin layer (latex) being about eighteen times higher than that of human skin. However, the peak was higher for the tested material properties than for that of the human tissue properties of finger indicating that the loss factors of human tissue (0.6) is higher than that found for latex (0.04).

Figure 8 shows the mode shapes of both FE models (human and tested materials), at the peak frequency and 400 Hz. In general, the strain distribution at resonance frequency appeared around the soft tissues of both models and was higher for the human one. At 400 Hz, the strain was found to be high at the finger sides. The skin layer was affected in the human model, unlike in the material model (see Figure 8 b) where the skin layer was not dynamically affected. As mentioned earlier, the material used in order to replicate the skin was eighteen times stiffer than the human skin. Also, both FE models at all conditions showed that the main artery regions of the finger (below the bone centre, at either side) were found to be most affected by vibration, which was considered to be one of the factors that may lead to vibration-induced white finger.

5. Discussion

Some studies have attempted to use artificial systems to replicate the mechanical behaviour of the human fingertip and have investigated many materials for the purpose of friction measurement and Young's modulus effects (Ramkumar et al., 2003a; b; Shao et al., 2009). To date, however, no experimental protocol has been developed to measure the effect of transmitted vibration into the soft tissues of the finger, using an artificial test-bed.

This study investigated two types of material (latex and silicone gel) in order to obtain similar mechanical properties to those of the real finger, including the Young's modulus and loss factors, and to discover how these properties can be affected when subjected to different strain rates and temperature change.

The DMA data obtained from testing represented the mechanical behaviour of the tested materials. The Young's modulus represents how the energy can be stored by materials under loading conditions, and how it affects the dynamic stiffness of materials tested. The loss factors represent the ratio of the energy dissipated to that stored and affect the damping properties of the materials specimens (ISO 6321-1, 1996).

DMA data obtained from two silicone specimens showed that the Young's modulus was within the range of interest and this was stable over a medium term for a range of dynamic strains and temperatures. Results allowed the appropriate mixing ratio to be selected in order to replicate the subcutaneous tissues of the human finger.

Even though the DMA data obtained from the latex specimen showed that its Young's modulus was considerably higher than that of the outer layer of skin, it was found to be the best material for replicating skin as it has the strength required and can adhere to other surfaces such as silicone gel. It was also found useful in keeping all parts of the finger model enclosed. The problems associated with the higher Young's modulus of latex material was reduced by decreasing the thickness of the skin layer.

The results obtained from FE modelling of the finger showed skin stiffness can affect the vibration behaviour of the finger. At resonance frequency the highest strain region was near location of the main arteries. This effect was higher for the human finger model than the artificial finger model. This indication was reported to be one of the factors that are linked to the occurrence of VWF syndromes.

It is hypothesised that the differences in transmissibility between the finger models and the human finger could be because the loss factors of the human tissues are higher than the gel, and the stiffness of the system is probably nonlinear (Kitazaki et al., 1995). Indicating that further work are required in order to validate vibration behaviour of the artificial model of the finger, using the human subjects.

This study provided a new protocol for developing and assessing the artificial test-bed of the finger to replicate the load-deflection behaviour of human finger, but with some limitations that need further examination including the difficulty to produce a homogenous thickness of the outer latex layer of the finger model. The latex material used was found to be about eighteen times stiffer than human skin. Thus, further alternative materials could be investigated to find a material that has mechanical properties closer to that of human skin. Also, the FE modelling to study the parameters of materials of both the human and the

artificial finger included a simplification of assumed symmetry. It is recommended these should be analysed further using 3D FE modelling of the finger's geometry in different sizes. This will provide a good comparison of the parameters, which may help in the design of future finger models.

6. Conclusions

The results show how DMA testing of the materials can be used to help in developing a reasonable physical model by finding a material with low sensitivity to temperature and dynamic strains. This technique allows the investigation of materials to replicate the mechanical behaviour of the human finger. The indentation measurement of the finger model showed the load-deflection behaviour was found to be within the range of that of the human finger.

A protocol for developing a reasonable artificial model to replicate the mechanical behaviour of the human finger has been established and can now be used in future experiments for assessing finger-transmitted vibrations. The model finger AF3 was selected as the best model for replicating loading behaviour similar to that found from human measurements.

The 2D FE modelling of the proximal finger segment used allows a good comparison between an FE model of the human finger and the artificial finger. This also provided a good understanding of finger-transmitted vibration and showed that the strain was found to be high around the artery regions of the finger.

This synthetic test-bed and protocol can now be used in future experiments for assessing finger-transmitted vibrations. It can help in assessing anti-vibration glove materials without the need for human subjects (which can sometimes be difficult due to ethical issues) and provide consistent control of test parameters such as grip force. Crucially, it also allows vibration to be measured inside the soft tissues.

Acknowledgements:

The authors wish to thank the Libyan Government for financial support for a PhD study and Jamie Booth and Leslie Morton for their technical support.

References

- Alexander, B. and K. Viktor (2010). "Proportions of Hand Segments." *International Journal of Morphology* 28(3): 755-758.
- Cheng, C. H., M. J. J. Wang and S. C. Lin (1999). "Evaluating the effects of wearing gloves and wrist support on hand-arm response while operating an in-line pneumatic screwdriver." *International Journal of Industrial Ergonomics* 24: 473-481.
- Concettoni, E. and M. Griffin (2009). "The apparent mass and mechanical impedance of the hand and the transmission of vibration to the fingers, hand, and arm." *Journal of Sound and Vibration* 325(3): 664-678.
- Derler, S., U. Schrade and L. C. Gerhardt (2007). "Tribology of human skin and mechanical skin equivalents in contact with textiles." *Wear* 263(7-12): 1112-1116.
- Dewangan, K. N., C. Owary and R. K. Datta (2010). "Anthropometry of male agricultural workers of north-eastern India and its use in design of agricultural tools and equipment." *International Journal of Industrial Ergonomics* 40(5): 560-573.

Dong, J. H., R. G. Dong, S. Rakheja, D. E. Welcome, T. W. McDowell and J. Z. Wu (2008). "A method for analyzing absorbed power distribution in the hand and arm substructures when operating vibrating tools." *Journal of Sound and Vibration* 311(3-5): 1286-1304.

Dong, R. G., T. W. McDowell, D. E. Welcome, C. Warren, Wu, J.Z., and S. Rakheja (2009). "Analysis of anti-vibration gloves mechanism and evaluation methods." 435-453 321.

Dong, R. G. W., Daniel E. McDowell, Thomas W. Wu, John Z. (2013). "Modeling of the biodynamic responses distributed at the fingers and palm of the hand in three orthogonal directions." *Journal of Sound and Vibration* 332(4): 1125-1140.

Eliot, G. (1991). *Human Anatomy for Artist*. New York, Oxford University press.

Griffin, M. J. (1990). *Handbook of Human Vibration*. London, Academic Press.

Griffin, M. J., C. R. Macfarlane and C. D. Norman (1982). *The transmission of vibration to the hand and the influence of gloves in: Vibration Effects on the Hand and Arm in Industry*. A. J. Brammer, W. Taylor., J. Wiley and Sons. New York.

Hewitt, S. (1998). "Assessing the performance of anti-vibration gloves—A possible alternative to ISO 10819, 1996." *The Annals of Occupational Hygiene* 42(4): 245-252.

ISO 5349-1 (2001). *Mechanical vibration — Measurement and evaluation of human exposure to hand-transmitted vibration — Part 1: General requirements*. Geneva, Switzerland, International Organization for Standardization.

ISO 6321-1 (1996). *Plastics - Determination of dynamic mechanical properties - Part 1:General principles*. Geneva, Switzerland, International Organization for Standardization.

ISO 10819 (1996). *Mechanical vibration and shock — hand-arm vibration — Method for the measurement and evaluation transmissibility of gloves at the palm of the hand*. Geneva, Switzerland, International Organization for Standardization.

ISO 10819 (2013). *Mechanical vibration and shock — Hand-arm vibration —Measurement and evaluation of the vibration transmissibility of gloves at the palm of the hand*. Geneva, Switzerland, International Organization for Standardization.

Kitazaki, S. and M. J. Griffin (1995). "A data correction method for surface measurement of vibration on the human body." *Journal of Biomechanics* 28(7): 885-890.

Maiti, R., L. C. Gerhardt, Z. S. Lee, R. A. Byers, D. Woods, J. A. Sanz-Herrera, S. E. Franklin, R. Lewis, S. J. Matcher and M. J. Carre (2016). "In vivo measurement of skin surface strain and sub-surface layer deformation induced by natural tissue stretching." *J Mech Behav Biomed Mater* 62: 556-569.

Paddan, G. S. and M. J. Griffin (2001). *Measurement of glove and hand dynamics using knuckle vibration*. 9th International Conference on Hand-Arm Vibration. Nancy, France.

Pan, L., L. Zan and F. Foster (1998). "Ultrasonic and viscoelastic properties of skin under transverse mechanical stress in vitro." *Ultrasound in Medicine and Biology* 24(7): 995-1007.

Ramkumar, S. S., D. J. Wood, K. Fox and S. C. Harlock (2003a). "Developing a Polymeric Human Finger Sensor to Study the Frictional Properties of Textiles Part I: Artificial Finger Development." *Textile Research Journal* 73(6): 469-473.

Ramkumar, S. S., D. J. Wood, K. Fox and S. C. Harlock (2003b). "Developing a Polymeric Human Finger Sensor to Study the Frictional Properties of Textiles Part II: Experimental Result." *Textile Research Journal* 73(7): 606-610.

- Shao, F., T. H. C. Childs and B. Henson (2009). "Developing an artificial fingertip with human friction properties." *Tribology International* 42(11-12): 1575-1581.
- Wagner, M. B., G. J. Gerling and J. Scanlon (2008). "Validation of a 3-D Finite Element Human Fingerpad Model Composed of Anatomically Accurate Tissue Layers." Department of Systems and Information Engineering, University of Virginia, USA: 101-105.
- Wang, Z., Y. Abe, S. Hirai and S. Morikawa (2011). "A 3D FE Dynamic Model of Human Fingertip Based on MRI Data." 1.
- Wang, Z., L. Wang, V. A. Ho, S. Morikawa and S. Hirai (2012). "A 3-D Nonhomogeneous FE Model of Human Fingertip Based on MRI Measurements." *IEEE Transactions on Instrumentation and Measurement* 61(12): 3147-3157.
- Welcome, D. E., R. G. Dong, X. S. Xu, M. Christopher, T. W. McDowell and J. Z. Wu (2011). "Investigation of the 3-D vibration transmissibility on the human hand –arm system using a 3-D scanning laser vibrometer." *Canadian Acoustics* 39: 44-45.
- Welcome, D. E., R. G. Dong, X. S. Xu, C. Warren and T. W. McDowell (2014). "The effects of vibration-reducing gloves on finger vibration." *International Journal of Industrial Ergonomics* 44(1): 45-59.
- Welcome, D. E., R. G. Dong, X. S. Xu, C. Warren, T. W. McDowell and J. Z. Wu (2015). "An examination of the vibration transmissibility of the hand-arm system in three orthogonal directions." *International Journal of Industrial Ergonomics* 45: 21-34.
- Wu, J. Z., R. G. Dong and D. E. Welcome (2006a). "Analysis of the point mechanical impedance of fingerpad in vibration." *Med Eng Phys* 28(8): 816-826.
- Wu, J. Z., R. G. Dong, D. E. Welcome and T. W. McDowell (2015). THREE-DIMENSIONAL FINITE ELEMENT MODELING OF THE EFFECTS OF GRIPPING FORCE ON FINGER VIBRATION TRANSMISSIBILITY. Thirteenth International Conference on Hand-Arm Vibration, Beijing, China, Beijing University Health Science Center Capital Medical University.
- Wu, J. Z., R. G. Dong, D. E. Welcome and X. S. Xu (2010). "A method for analyzing vibration power absorption density in human fingertip." *Journal of Sound and Vibration* 329(26): 5600-5614.
- Wu, J. Z., K. Krajnak, D. E. Welcome and R. G. Dong (2006b). "Analysis of the dynamic strains in a fingertip exposed to vibrations: Correlation to the mechanical stimuli on mechanoreceptors." *J Biomech* 39(13): 2445-2456.
- Wu, J. Z., K. Krajnak, D. E. Welcome and R. G. Dong (2008). "Three-dimensional finite element simulations of the dynamic response of a fingertip to vibration." *J Biomech Eng* 130(5): 054501.
- Wu, J. Z., D. E. Welcome, K. Krajnak and R. G. Dong (2007). "Finite element analysis of the penetrations of shear and normal vibrations into the soft tissues in a fingertip." *Medical Engineering and Physics* 29: 718-727.
- Zheng, Y. and A. F. Mak (1996). "An ultrasound indentation system for biomechanical properties assessment of soft tissues in-vivo." *IEEE Transactions on Biomedical Engineering* 43(9): 912-918.

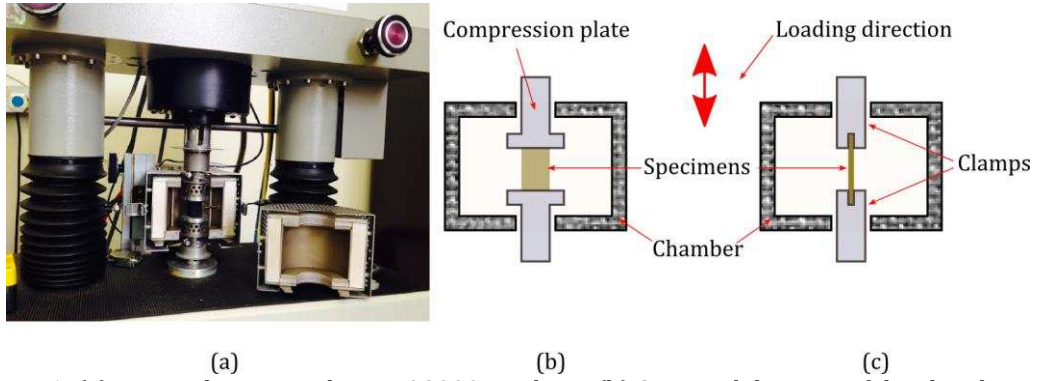


Figure 1: (a) Metravib Viscoanalyser VA2000 machine; (b) Sectional diagram of the chamber and specimens when using compression plates; (c) tension modes using clamps.

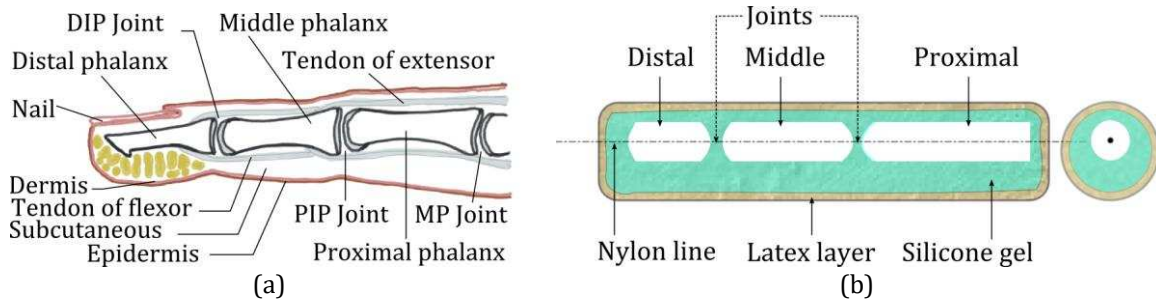


Figure 2: (a) anatomy of the human index finger; (b) structure of artificial model of the finger.

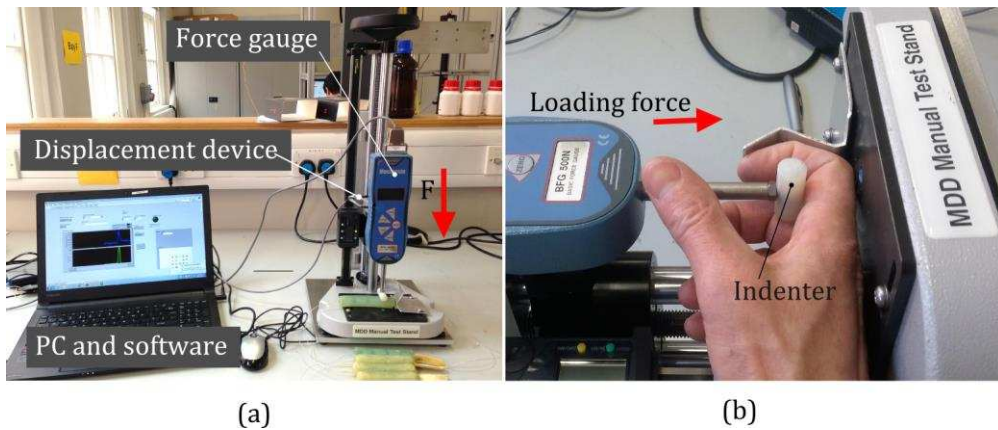


Figure 3: The experiment set-up for indentation measurement

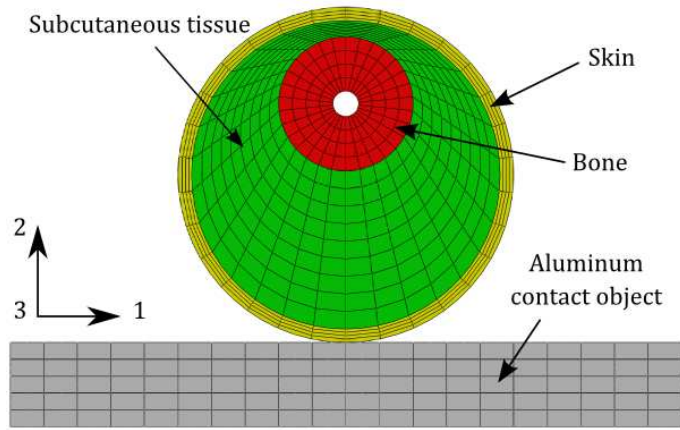


Figure 4: 2D finite element model of an index finger proximal in contact with an aluminium plate

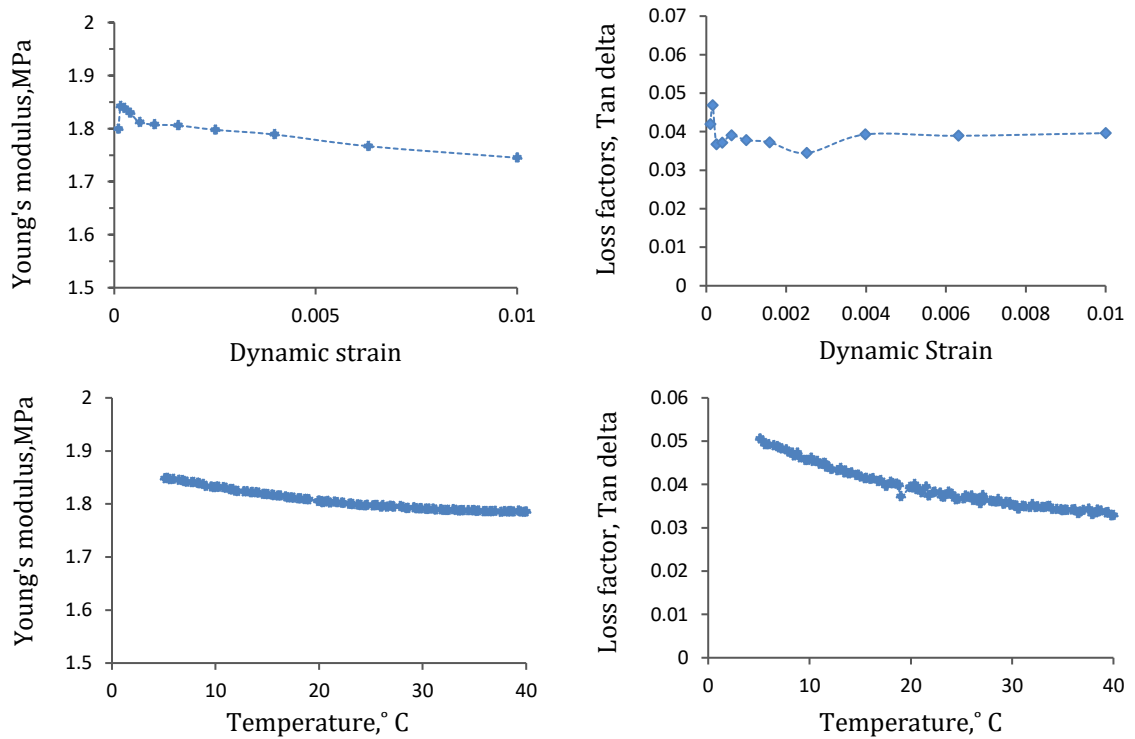


Figure 5: Young's modulus and loss factors against dynamic strain and temperature of latex specimen

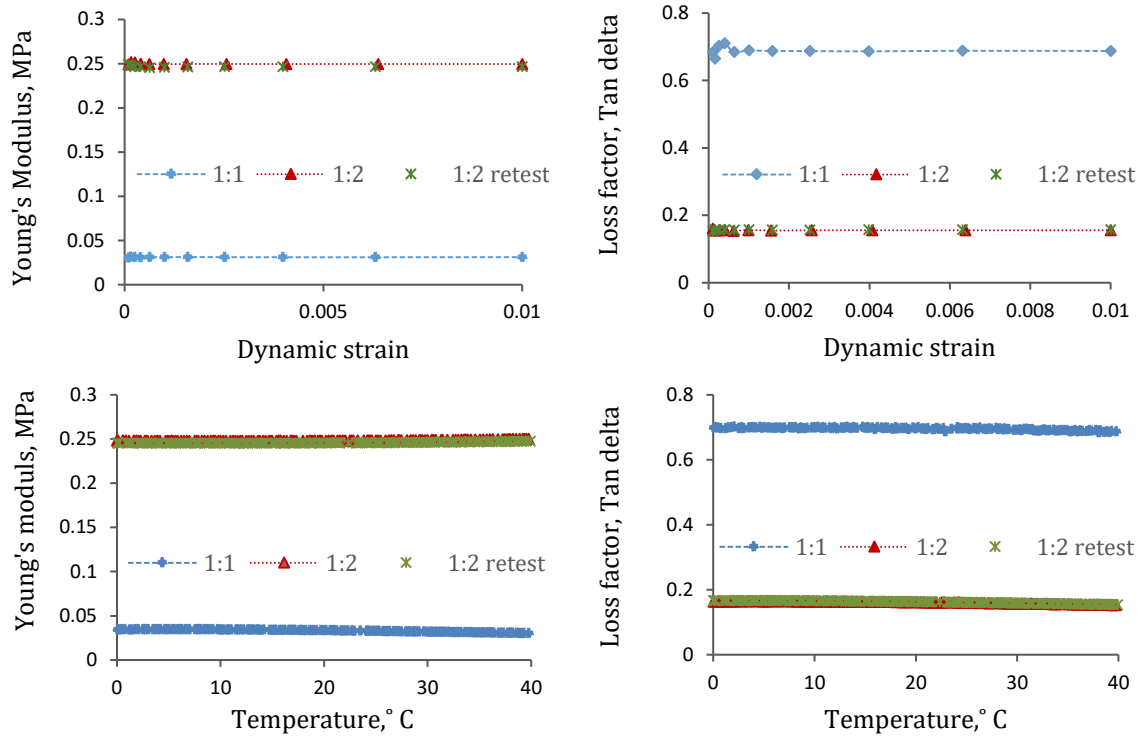


Figure 6: Young's modulus and loss factors against dynamic strain and temperature of silicone gel specimens

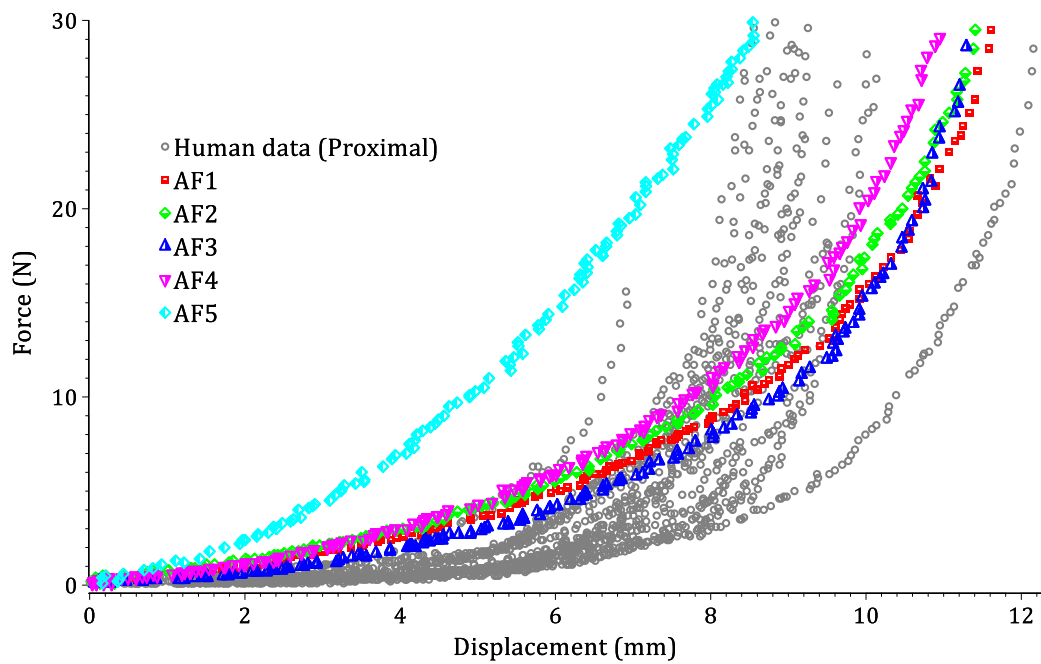


Figure 7: The load-deflection behaviour of the finger model 3 and the human right index finger

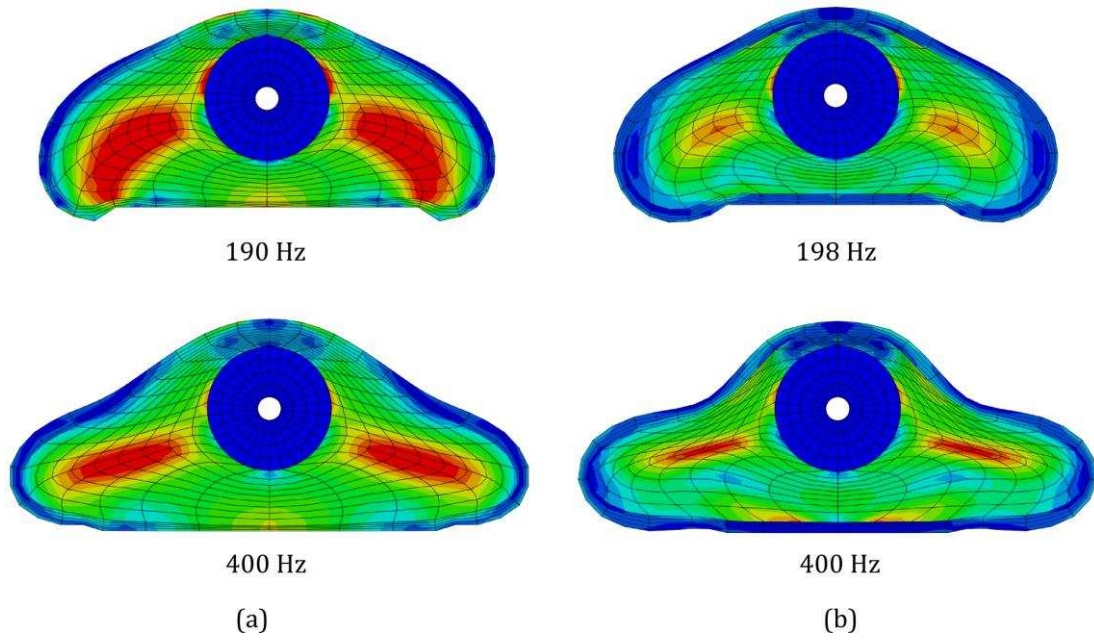


Figure 8: Mode shapes of FE models at resonance frequency and 400 Hz, during a deflection of 6 mm toward the handle: a) when human tissue parameters were applied; b) using parameters from tested materials